Disruption of $GABA_A$ Receptors on GABAergic Interneurons Leads to Increased Oscillatory Power in the Olfactory Bulb Network

ZOLTAN NUSSER,[1,3] LESLIE M. KAY,[2,5] GILLES LAURENT,[2] GREGG E. HOMANICS,[4] AND ISTVAN MODY[1]
[1]*Department of Neurology, UCLA School of Medicine, Los Angeles 90095-1769;* [2]*Biology Division, California Institute of Technology, Pasadena, California 91125;* [3]*Laboratory of Cellular Neurophysiology, Institute of Experimental Medicine, Hungarian Academy of Sciences, 1083 Budapest, Hungary;* [4]*Departments of Anesthesiology and Pharmacology, University of Pittsburgh School of Medicine, Pittsburgh, Pennsylvania 15260; and* [5]*Department of Psychology, Institute for Mind and Biology, University of Chicago, Chicago, Illinois 60637*

Received 19 April 2001; accepted in final form 7 September 2001

Nusser, Zoltan, Leslie M. Kay, Gilles Laurent, Gregg E. Homanics, and Istvan Mody. Disruption of $GABA_A$ receptors on GABAergic interneurons leads to increased oscillatory power in the olfactory bulb network. *J Neurophysiol* 86: 2823–2833, 2001. Synchronized neural activity is believed to be essential for many CNS functions, including neuronal development, sensory perception, and memory formation. In several brain areas $GABA_A$ receptor–mediated synaptic inhibition is thought to be important for the generation of synchronous network activity. We have used $GABA_A$ receptor β3 subunit deficient mice ($\beta3-/-$) to study the role of GABAergic inhibition in the generation of network oscillations in the olfactory bulb (OB) and to reveal the role of such oscillations in olfaction. The expression of functional $GABA_A$ receptors was drastically reduced (>93%) in $\beta3-/-$ granule cells, the local inhibitory interneurons of the OB. This was revealed by a large reduction of muscimol-evoked whole-cell current and the total current mediated by spontaneous, miniature inhibitory postsynaptic currents (mIPSCs). In $\beta3-/-$ mitral/tufted cells (principal cells), there was a two-fold increase in mIPSC amplitudes without any significant change in their kinetics or frequency. In parallel with the altered inhibition, there was a significant increase in the amplitude of theta (80% increase) and gamma (178% increase) frequency oscillations in $\beta3-/-$ OBs recorded in vivo from freely moving mice. In odor discrimination tests, we found $\beta3-/-$ mice to be initially the same as, but better with experience than $\beta3+/+$ mice in distinguishing closely related monomolecular alcohols. However, $\beta3-/-$ mice were initially better and then worse with practice than control mice in distinguishing closely related mixtures of alcohols. Our results indicate that the disruption of $GABA_A$ receptor–mediated synaptic inhibition of GABAergic interneurons and the augmentation of IPSCs in principal cells result in increased network oscillations in the OB with complex effects on olfactory discrimination, which can be explained by an increase in the size or effective power of oscillating neural cell assemblies among the mitral cells of $\beta3-/-$ mice.

INTRODUCTION

Sensory stimulus associated oscillatory synchronization has been described in the olfactory (Adrian 1942, 1950; Bressler and Freeman 1980; Freeman 1975, 1976; Gelperin and Tank 1990; Gray and Skinner 1988; Laurent and Davidowitz 1994; MacLeod and Laurent 1996; Stopfer et al. 1997) and visual (Engel et al. 1997; Gray and Singer 1989) systems of many species. The role of such synchronization is still debated, but several recent studies have provided strong evidence for the essential role of oscillatory synchronization in olfactory information coding in invertebrates (e.g., locust and honeybee). In the locust, information about odor identity is carried not only by the "spatial" component of the active neuronal ensemble, but also by the precise timing of action potential firing (Laurent and Davidowitz 1994; MacLeod and Laurent 1996; Wehr and Laurent 1996). It has been shown in honeybees that odor encoding involves the oscillatory synchronization of an ensemble of projection neurons (PN), and that their desynchronization results in impaired discrimination of molecularly similar odorants, but not that of dissimilar odorants (Stopfer et al. 1997). In locusts, PN desynchronization also leads to a loss of tuning specificity in neurons found two synapses downstream of the PNs, further implicating neuronal synchronization as being a functionally relevant parameter of neuronal activity (MacLeod et al. 1998). Oscillatory synchronization in the gamma, beta, and theta frequency ranges has been described in the olfactory bulb and piriform cortex of mammals (Adrian 1950; Bressler and Freeman 1980; Freeman 1975; Kay and Freeman 1998), but its role in sensory coding is still unclear. This is mainly due to the lack of experimental tools allowing the selective alteration of oscillatory synchronization in a defined part of the olfactory pathway in vivo without modifying the responsiveness of neurons to naturally occurring stimuli and their spatial arrangements.

In several mammalian and nonmammalian species, oscillatory synchronization of some neural populations requires intact $GABA_A$ receptor–mediated synaptic inhibition (reviewed by Buzsaki and Chrobak 1995; Singer 1996; Traub et al. 1998). All nerve cells in the mammalian brain express several subunits of the $GABA_A$ receptor (Fritschy and Mohler 1995; Wisden et al. 1992), which are usually co-assembled into several $GABA_A$ receptor subtypes. Granule cells in the olfactory bulb express only the β3 variant of the β subunit, whereas mitral and tufted cells express all three known β subunits (β1, β2, and β3) (Laurie et al. 1992; Nusser et al. 1999b). Because β subunits are essential for the formation of functional $GABA_A$

Address for reprint requests: Z. Nusser, Lab. of Cellular Neurophysiology, Institute of Experimental Medicine, Hungarian Academy of Sciences, Szigony St. 43, 1083 Budapest, Hungary (E-mail: nusser@koki.hu).

The costs of publication of this article were defrayed in part by the payment of page charges. The article must therefore be hereby marked "*advertisement*" in accordance with 18 U.S.C. Section 1734 solely to indicate this fact.

 0022-3077/01 $5.00 Copyright © 2001 The American Physiological Society

receptors, we predicted that after the genetic deletion of the β3 subunit gene (Homanics et al. 1997) functional $GABA_A$ receptors would be altered in a cell type–specific manner in the olfactory bulb. Namely, we predicted a considerable reduction of functional $GABA_A$ receptors in granule cells, the local circuit GABAergic interneurons of the bulb, without a large reduction in principal cells (mitral/tufted cells). Previous experimental and modeling studies indicated that disruption of $GABA_A$ receptor–mediated inhibition between GABAergic local circuit interneurons results in the loss of gamma frequency oscillations in the hippocampus and neocortex (Tamas et al. 2000; Traub et al. 1996; Wang and Buzsaki 1996; Whittington et al. 1995), but it could also lead to hyper-synchrony in the thalamus (Huntsman et al. 1999). Thus in the present study, we used $GABA_A$ receptor β3 subunit deficient mice to study the role of GABAergic synaptic inhibition of granule cells in oscillatory synchronization in the mammalian olfactory bulb and to examine the possible consequences of altered neuronal synchronization on olfaction.

METHODS

Slice preparation and in vitro electrophysiological recordings

One 28-day-old and four adult (>3 month old) $\beta3-/-$ mice (DeLorey et al. 1998; Homanics et al. 1997) and four adult $\beta3+/+$ mice were anesthetized with halothane before decapitation in accordance with the guidelines of the UCLA Office for Protection of Research Subjects. The brains were then removed and placed into an ice-cold artificial cerebrospinal fluid (ACSF) containing (in mM) 126 NaCl, 2.5 KCl, 2 $CaCl_2$, 2 $MgCl_2$, 1.25 NaH_2PO_4, 26 $NaHCO_3$, and 10 D-glucose, pH 7.3 when bubbled with 95% O_2-5% CO_2. The olfactory bulb was glued to a platform, and 300-μm-thick sagittal slices were cut with a Vibratome (Leica VT1000S). The slices were stored submerged at 32°C in ACSF until they were transferred to the recording chamber. During recording, the slices were continuously perfused with 33–36°C ACSF containing 3–5 mM kynurenic acid (Sigma) and 0.7 μM tetrodotoxin (Calbiochem, La Jolla, CA). All recordings were made from the somata of visually identified neurons (Zeiss Axioscope and Leica DMS IR-DIC videomicroscopy, ×40 water immersion objective) with an Axopatch 200B amplifier (Axon Instruments, Foster City, CA). Patch electrodes were pulled (Narishige PP-83, Tokyo) from thick-walled borosilicate glass (1.5 mm OD, 0.86 mm ID, Sutter Instruments, Novato, CA) and were filled with a solution containing (in mM) 140 CsCl, 4 NaCl, 1 $MgCl_2$, 10 HEPES, 0.05 EGTA, 2 Mg-ATP, and 0.4 Mg-GTP. All solutions were titrated to a pH of 7.25 and an osmolarity of 280–290 mosmol. The DC resistance of the electrodes was 2–8 MΩ when filled with pipette solution. Series resistance and whole cell capacitance were estimated by compensating for the fast current transients evoked at the onset and offset of 8-ms, 5-mV voltage-command steps and were checked every 2 min during the recording. If the series resistance increased by more than 50%, the recording was discontinued. The series resistance remaining after 75–80% compensation (with 7- to 8-μs lag values) was 1.4 ± 0.07 and 1.7 ± 0.26 (SE) MΩ for $\beta+/+$ and $\beta3-/-$ mitral cells, respectively; and 3.9 ± 0.3 and 3.8 ± 0.4 MΩ for $\beta+/+$ and $\beta3-/-$ granule cells, respectively. Data are expressed as means ± SE and are compared with an unpaired *t*-test assuming unequal variances unless otherwise stated.

Analysis of the in vitro electrophysiological data

All recordings were low-pass filtered at 2 kHz and digitized on-line at 20 kHz, as described earlier (Nusser et al. 1999b). In-house data acquisition and analysis software (written in LabView, National Instruments, Austin, TX) was used to measure the amplitudes, 10–90% rise times, 67% decay times and charge transferred by miniature inhibitory postsynaptic currents (mIPSCs). The decay of the averaged currents was fitted with a single or the sum of two exponential functions. The weighted decay time from the exponential fit [$\tau_{w(f)}$] was calculated as $\tau_{w(f)} = \tau_1 * A_1 + \tau_2 * (1 - A_1)$, where τ_1 and τ_2 are the fast and slow decay time constants, respectively, and A_1 is the contribution of the first exponential to the amplitude. The weighted decay time constant from the area [$\tau_{w(a)}$] was calculated by dividing the area of each mIPSC by its peak amplitude.

In vivo recordings from freely moving animals

Four control and three $\beta3-/-$ mice were anesthetized with 100 mg/kg ketamine and 5 mg/kg xylazine. The skin was opened and small holes (~2 mm) were drilled in the skull. Following the opening of the dura mater, a bipolar electrode (twisted 60-μm tungsten wires with vertical tip separation of ~0.5 mm) was lowered into the dorsal surface of the left olfactory bulb. A stainless steel watch screw was driven into the skull above the cerebellum to serve as a ground electrode. All electrodes were stabilized with dental cement. During surgery and postoperative care, all efforts were made to comfort the animals, in accordance with the guidelines of the UCLA Office for Protection of Research Subjects.

Two days after the surgery, electroencephalograms were low-pass filtered at 200 Hz and digitized at 1 kHz using a data acquisition board (PCI-MIO 16E-4, National Instruments, Austin, TX) and in-house data acquisition software written in LabView (National Instruments). Power spectra and autocorrelograms were computed with LabView. The power spectra were normalized in two ways. *1*) The power spectra during both immobility and exploration were normalized to the maximum of the lowest frequency peak during immobility (its value defined as 1). *2*) The power spectra were normalized to a mean of 0 and a SD of 1. Almost identical results were obtained with both normalizations, but as the latter method resulted in greater variance within conditions, we have chosen to present our data with the first way of normalization. We discriminated between two behavioral states of the animals during the recordings: immobility, during which the animals did not move and showed no observable sign of sniffing; and exploration, during which the animals moved around in their cage and showed intense sniffing activity.

Odor discrimination

All mice (4 adult $\beta3+/+$ and 4 adult $\beta3-/-$ mice) were trained using a protocol developed and modified according to Linster and Hasselmo (1999) and is as presented elsewhere (Kay et al. 2000). Mice were first introduced to the test arena (polycarbonate box similar to the home cage and fitted with a dividing door). They were trained to dig in a small glass dish of sand for a food reward until they reached criterion (initiating digging within 10 s). They were then presented with two dishes, one scented (5 drops of 5% odorant in mineral oil, mixed into the sand) and one unscented (5 drops of mineral oil). The animals learned to dig in the scented dish for a reward.

Odor testing sessions began with 10 training trials, in which the mouse learned to dig in response to the training odor (hexanol or an alcohol mixture) and avoid digging in the control dish. The mouse was then tested on a set of odors in random order, including the learned odor. Each test trial was 20 s long, after which the animal was removed from the arena. In the test trials, there was no reward present in the dish, and the amounts of time spent digging in the odor dish (digging time) and the control dish were measured. To avoid behavioral extinction, the mouse was given one to three reinforcement trials with the trained odor in between unrewarded test trials. In the first experiment, test odors were alcohols of various chain lengths (3-C to 8-C and 10-C) and one nonalcohol, isoamyl acetate (IAA). The

training odor was hexanol (6-C). All odorants were 5% solutions in mineral oil. The odorants were tested twice in each session (*round 1* and *round 2* in Fig. 7). Generalization was measured as significant digging in an odor other than the training odor.

In the second experiment the four β3+/+ mice and three of the original four β3−/− mice were challenged with a more difficult odor identification task. The training odor in these sessions was a 5% dilution in mineral oil of a mixture of alcohols (OM: butanol, pentanol, heptanol, and decanol). The test odors were the original mixture and four mixtures consisting of three of the four alcohols in the original mixture (M1: pentanol, heptanol, and decanol; M2: butanol, heptanol, and decanol; M3: butanol, pentanol, and decanol; M4: butanol, pentanol, and heptanol). The mice were tested as before, and digging times were recorded for each test mixture and the control dishes. The odorants were tested three times (*rounds 1–3* in Fig. 8). Due to the small number of animals and the variability of digging durations across animals, data were normalized by transformation to their *Z*-scores. Normalized digging times for each test odor were compared in a one-way ANOVA across test odors. The test odor digging times were then compared with each other using a post hoc Newman-Keuls test. Values of $P < 0.05$ were considered significant. Only digging times in the test odors were analyzed, as the mice rarely dug in the control sand.

Immunohistochemistry

Light microscopic immunostaining for $GABA_A$ receptor subunits was performed as described previously (Nusser et al. 1995). Olfactory bulbs from a control and a β3−/− mouse were removed and placed into ice-cold fixative containing 4% paraformaldehyde, 0.05% glutaraldehyde, and ~0.2% picric acid made up in 0.1 M phosphate buffer (PB, pH 7.4) for 50 min. Vibratome sections (sagittal, 70 μm in thickness) were cut and collected in PB. Normal goat serum (20%) was used in 50 mM Tris-HCl (pH 7.4) containing 0.9% NaCl (TBS) as the blocking solution for 0.5 h followed by the incubation with purified primary antibodies diluted in TBS containing 1% normal goat serum and 0.05% Triton X-100 overnight. The primary antibodies were used at the following final concentrations: β1 [code No. β1(350–404)R16/6] (Jechlinger et al. 1998), 1.25 μg protein/ml; β2 [code No. β2(351–405)R20] (Jechlinger et al. 1998), 1.9 μg/ml; and β3 [code No. β3(345–408)R21] (Slany et al. 1995), 1 μg/ml. After washing, the sections were incubated for 90 min in biotinylated secondary antibodies (diluted 1:50 in TBS; Vector Lab., Burlingame, CA), followed by further washings and incubation in avidin biotinylated horseradish peroxidase complex (1:100 dilution in TBS) for 2 h. Peroxidase enzyme reaction was carried out with 3,3′-diaminobenzidine tetrahydrochloride as chromogen and H_2O_2 as oxidant. The sections were then routinely processed for light microscopic examination (Somogyi et al. 1989).

RESULTS

Alteration of GABAergic synaptic neurotransmission in the olfactory bulb

First, we recorded mIPSCs from granule cells of the olfactory bulb in the presence of the ionotropic glutamate receptor blocker kynurenic acid (3–5 mM) and the sodium channel blocker tetrodotoxin (0.7 μM) under whole-cell voltage-clamp configuration in acute brain slices. Because granule cells were held at −70 mV and because symmetrical Cl^- concentrations were used, $GABA_A$ receptor–mediated mIPSCs were inward. In agreement with our previous studies (Hajos et al. 2000; Nusser et al. 1999b) in control mice, mIPSCs occurred relatively infrequently (1.16 ± 0.30 Hz, $n = 7$), had an average amplitude of 74.8 ± 11.9 pA, a weighted decay time constant of 8.3 ± 0.6 ms and the charge carried by each mIPSC was 0.68 ± 0.12 pC (Fig. 1). In β3−/− mice, there was an ~80% reduction in mIPSC frequency (from 1.16 ± 0.30 Hz to 0.24 ± 0.04 Hz, $n = 7$, $P = 0.01$, unpaired *t*-test) with an accompanying decrease in the amplitude (43% reduction, from 74.8 ± 11.9 pA to 42.9 ± 8.2 pA, $P = 0.02$) and decay time (42% reduction, 8.3 ± 0.6 ms in control and 4.8 ± 0.4 ms in β3−/−, $P < 0.001$). As a consequence, the total current entering through synaptic $GABA_A$ receptors was reduced by 93% ($P < 0.01$) in β3−/− mice compared with the controls (Fig. 1). To test whether the observed reduction in GABAergic synaptic currents was due to a decrease in surface $GABA_A$ receptors, we bath applied ~100 μM muscimol, a $GABA_A$ receptor agonist,

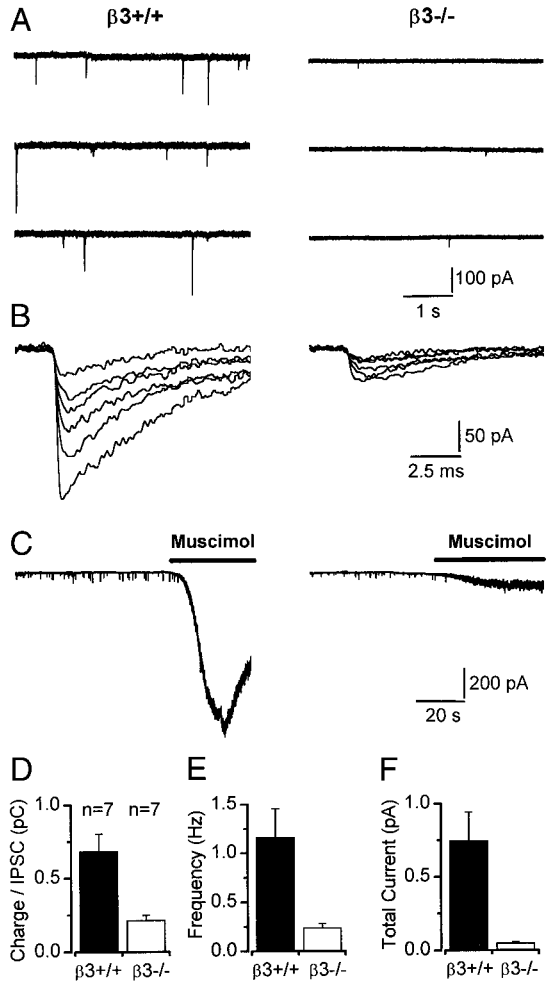

FIG. 1. Reduction of $GABA_A$ receptor–mediated inhibition in β3−/− granule cells. *A*: continuous 15-s recordings of spontaneous activity in a β3+/+ (*left panel*) and a β3−/− (*right panel*) animal in the presence of 3 mM kynurenic acid and 0.7 μM tetrodotoxin. Note that the frequency and the amplitude of the inward currents are greatly reduced. *B*: the 1st 6 consecutive miniature inhibitory postsynaptic currents (mIPSCs) from *A* are shown superimposed on an extended time scale. Note that the synaptic events in β3−/− granule cells have smaller amplitudes and faster decay times. *C*: approximately 100 μM muscimol evokes a much smaller current in β3−/− (*right panel*) than in control (*left panel*) granule cells. *D–F*: the 69% reduction (from 0.682 ± 0.123 pC to 0.125 ± 0.035 pC, $n = 7$, $P < 0.01$, unpaired *t*-test) in the charge transfer by mIPSCs together with an 80% reduction (from 1.16 ± 0.30 Hz to 0.24 ± 0.04 Hz, $n = 7$, $P = 0.01$, unpaired *t*-test) in mIPSC frequency resulted in a 93% reduction (from 0.745 ± 0.199 pA to 0.050 ± 0.009 pA, $n = 7$, $P < 0.01$, unpaired *t*-test) in the total current entering through $GABA_A$ receptors in β3−/− granule cells.

and recorded the drug-evoked whole-cell currents. As shown in two representative cells in Fig. 1*C*, muscimol evoked a much smaller inward current in $\beta3-/-$ granule cells compared with controls. As we did not use rapid agonist application, we did not attempt to quantify the results of these experiments.

Taken together, these results suggest that there was a great reduction in the expression of functional $GABA_A$ receptors on the surface of $\beta3-/-$ granule cells. However, it is clear that there is no complete loss of functional $GABA_A$ receptors from the surface of granule cells. Using immunocytochemistry with subunit-specific antibodies, we tested whether a compensatory up-regulation of other β subunits could explain the incomplete loss of synaptic currents. In control granule cells, similar to our previously published data (Nusser et al. 1999b), no immunoreactivity for the $\beta1$ and $\beta2$ subunits could be detected, but very strong staining for the $\beta3$ subunit was observed (Fig. 2). In the external plexiform layer, all three β subunit variants were strongly expressed. There was no detectable staining for the $\beta3$ subunit in the whole brain of $\beta3-/-$ mice, including the olfactory bulb, in agreement with the results of previous studies showing a complete loss of the $\beta3$ subunit (DeLorey et al. 1998). We could not detect any significant labeling for the $\beta1$ or $\beta2$ subunits in $\beta3-/-$ granule cells, whereas these subunits were strongly expressed in mitral/tufted cells.

To assess the effect of the $\beta3$ subunit gene deletion on GABAergic synaptic currents recorded in the principal cells of the olfactory bulb (mitral and tufted cells), mIPSCs were pharmacologically isolated and were recorded under whole-cell voltage-clamp. In control mitral cells, mIPSCs occurred with a frequency of 2.3 ± 0.8 Hz ($n = 9$) and had amplitudes of 42.9 ± 4.9 pA at -70 mV. The decay of the currents could be described either with a single exponential ($\tau = 3.7$ ms, $n = 6$ cells) or with the sum of two exponentials [$\tau_1 = 2.5$ ms (80%), $\tau_2 = 9.9$ ms, $n = 3$ cells]. In $\beta3-/-$ mitral cells, there was no significant change in the frequency of the synaptic currents (2.4 ± 0.7 Hz, $P > 0.05$ compared with controls; Fig. 3). The most parsimonious explanation of this result is that there is no change in the number of GABAergic synapses on mitral/tufted cells, consistent with the expression of additional β subunits ($\beta1$ and $\beta2$) in these cells. However, we observed a significant increase (118%) in the amplitude of mIPSCs (from 42.9 ± 4.9 pA to 93.4 ± 18.9 pA, $n = 9$, $P = 0.01$, Fig. 3) in $\beta3-/-$ mitral/tufted cells without any significant change in their kinetics [$\tau_{w(f)} = 3.7 \pm 0.2$ ms in control and $\tau_{w(f)} = 4.3 \pm 0.4$ ms in $\beta3-/-$, $P > 0.05$].

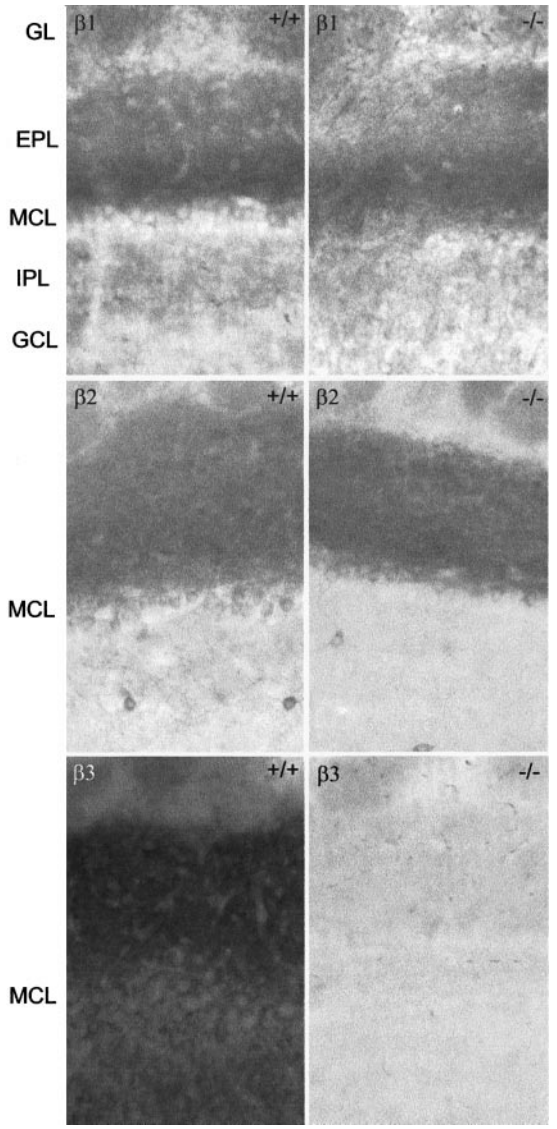

FIG. 2. Immunohistochemical demonstration of the distribution of the $\beta1$ (*top panels*), $\beta2$ (*middle panels*), and $\beta3$ (*bottom panels*) subunits in $\beta3+/+$ (*left panels*) and $\beta3-/-$ (*right panels*) mice. *Top panels*: no significant difference was seen in the expression of the $\beta1$ subunit in control and $\beta3-/-$ mice. In both animals, the $\beta1$ subunit is strongly expresses in the inner half and is weaker in the outer half of the external plexiform layer (EPL). The glomerular layer (GL) also shows some moderate labeling. The internal plexiform layer (IPL) and the granule cell layer (GCL) are very weakly stained, which is at the level of the nonspecific staining. *Middle panels*: the distribution of the $\beta2$ subunit is also very similar in both animals. The EPL is uniformly and strongly stained. In the GCL, only the short axon cells are labeled. *Bottom panels*: immunostaining for the $\beta3$ subunit is completely disappeared in $\beta3-/-$ mice, whereas it is very strong in all layers of the OB of control mice. MCL: mitral cell layer; all pictures at the same magnification (×185).

Effect of altered synaptic inhibition on network oscillations

To assess the role of GABAergic synaptic inhibition in the generation of synchronous network activity of the olfactory bulb, we recorded electroencephalograms (EEG) from the dorsal surface of the olfactory bulb of freely moving control and $\beta3-/-$ mice (Kay and Freeman 1998). We discriminated two behavioral states: *1*) immobility, periods during which the animals did not move, and no sign of sniffing was observed; and *2*) exploration, during which the animals explored their cage, and prominent sniffing activity was apparent. In control mice, during immobility, a prominent breathing-associated theta band (2–12 Hz) oscillation was apparent as described in several other species (Freeman 1976; Kay and Freeman 1998). By examining the power spectra of EEG recorded during immobility, we observed two peaks in the theta frequency band with frequencies of 4.2 ± 0.9 Hz and 9.7 ± 1.8 Hz, respectively (Figs. 4 and 6). During exploration, the lower frequency (2.5 ± 0.3 Hz) theta oscillation had smaller power ($41 \pm 8\%$ of control) than that during immobility, but the power of the higher frequency theta oscillation (6.7 ± 0.5 Hz) was almost identical to that in immobility (normalized power 0.51 ± 0.2 during immobility and 0.50 ± 0.11 during exploration). In control mice, gamma frequency oscillations were readily observed in both behavioral states with only slightly different

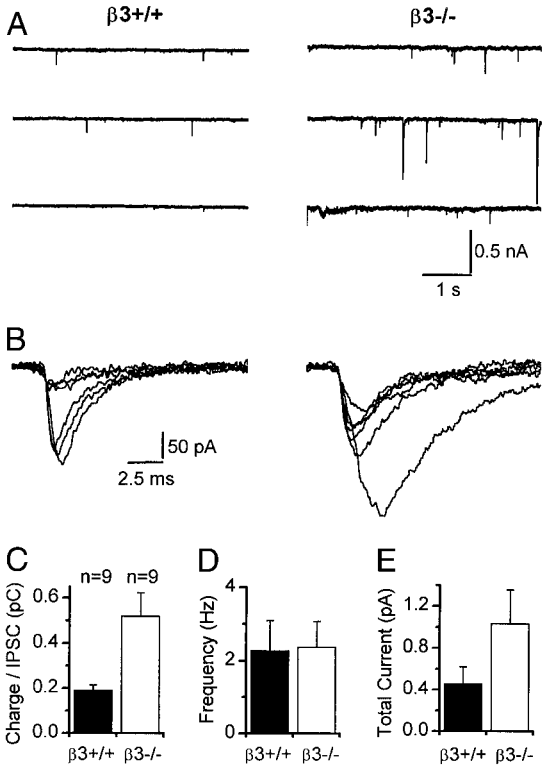

FIG. 3. Increased synaptic inhibition in β3−/− mitral cells. *A*: 15 s of continuous recordings of spontaneous $GABA_A$ receptor–mediated mIPSCs in β3+/+ (*left panel*) and β3−/− (*right panel*) mitral cells. There is a large increase in the amplitude of mIPSCs with an apparent increase in the frequency of the events. *B*: 6 consecutive mIPSCs are shown on extended time scales. Note the increased amplitude of the synaptic currents without any significant change in the time course of the events. *C*: the charge carried by the synaptic currents increased from 0.19 ± 0.03 pC to 0.52 ± 0.11 pC ($n = 9$; $P < 0.01$, unpaired *t*-test) in β3−/− mitral cells. *D* and *E*: as there was no significant change in the frequency of mIPSCs (2.27 ± 0.82 Hz in control and 2.37 ± 0.71 Hz in β3−/−, $n = 9$, $P = 0.46$, unpaired *t*-test), the 118% increase in the amplitude resulted in a similar increase (129% from 0.45 ± 0.16 pA to 1.03 ± 0.33 pA, $n = 9$, $P = 0.07$, unpaired *t*-test) in the total $GABA_A$ receptor–mediated synaptic current.

frequencies and power (Figs. 4 and 6; immobility: frequency = 43 ± 5 Hz, normalized power = 0.33 ± 0.17; exploration: frequency = 52 ± 5 Hz, normalized power = 0.36 ± 0.13), similar to that seen in rats (Kay and Freeman 1998). The most striking difference in the EEG patterns between control and β3−/− mice was the very pronounced power increase in the gamma frequency band in β3−/− animals (Figs. 5 and 6). During exploration, the normalized power (see METHODS) in gamma frequency band was increased almost threefold (normalized power: 0.36 ± 0.13 in control, $n = 4$; and 1.00 ± 0.10 in β3−/−, $n = 3$; $P < 0.01$, unpaired *t*-test), whereas the oscillation frequency remained unchanged (52 ± 5 Hz in control and 52 ± 3 Hz in β3−/−). We also compared the area under the nonnormalized power spectra between 40 and 80 Hz and found a very similar increase (320%) in β3−/− mice. During immobility, the power of the gamma frequency band was also greater in β3−/− mice, but this increase did not reach significance (normal power: 0.33 ± 0.17 in control, $n = 4$; and 0.60 ± 0.15 in β3−/−, $n = 3$; $P = 0.15$, unpaired *t*-test). During immobility, there was no significant change in either the frequency or the normalized power of the two theta frequency bands in β3−/− mice compared with controls (frequency: 4.3 ± 0.9 Hz, $n = 4$ vs. 3.0 ± 0 Hz, $n = 3$, $P = 0.14$ and 9.7 ± 1.8 Hz, $n = 4$ vs. 7.0 ± 1.0 Hz, $n = 3$, $P = 0.14$; normalized power for the higher frequency band: 0.51 ± 0.20, $n = 4$ vs. 0.78 ± 0.24, $n = 3$, $P = 0.22$ unpaired *t*-test). During exploration, however, the lower frequency theta oscillation had a significantly higher power (0.41 ± 0.08, $n = 4$ vs. 0.75 ± 0.09, $n = 3$, $P = 0.02$) with similar frequencies (2.5 ± 0.3 Hz, $n = 4$ vs. 4.3 ± 0.9 Hz, $n = 3$, $P > 0.05$) in β3−/− mice compared with controls. The higher frequency theta oscillation had a higher frequency (6.8 ± 0.5, $n = 4$ vs. 8.7 ± 0.3, $n = 3$, $P = 0.01$) and power (0.5 ± 0.1, $n = 4$ vs. 0.9 ± 0.16, $n =$

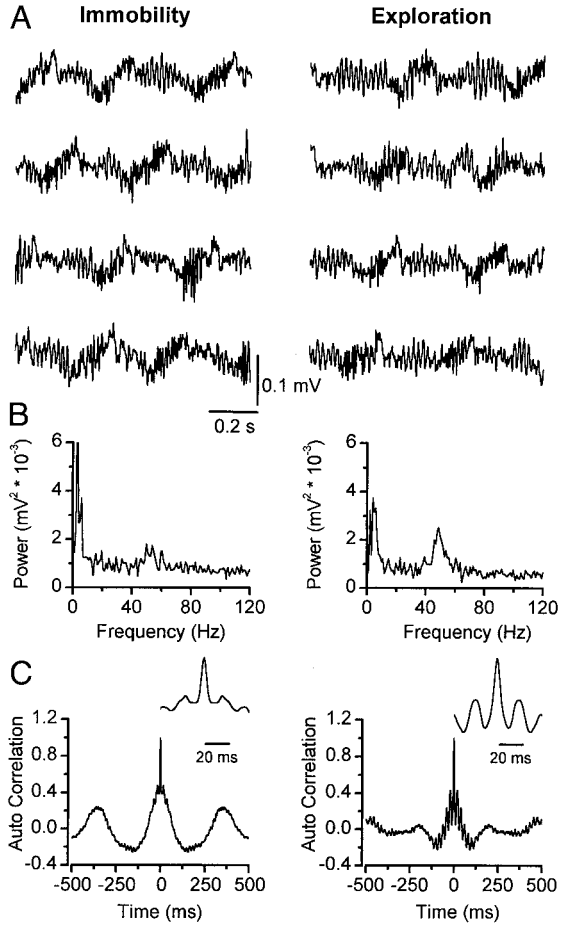

FIG. 4. Characterization of the rhythmic activity of the electroencephalogram recorded in vivo from the left olfactory bulb of a control mouse. *A*: 4 s of recordings during immobility (*left panel*) and exploration (*right panel*) using bipolar tungsten electrodes implanted into the surface of the dorsal olfactory bulb. There is a dominant low-frequency (~3 Hz) breathing-associated oscillatory behavior during immobility, which is the most prominent peak on the power spectrum (*B*) and dominates the autocorrelogram (*C*) as well. There is only a very weak gamma frequency oscillation during immobility, which is much stronger during exploration. *B*: there are 3 peaks in the power spectrum during both immobility (*left panel*) and exploration (*right panel*). During immobility, the most prominent peak is at ~3 Hz followed by a peak at approximately 6 Hz and a very small peak at 54 Hz. During exploration, the power of the low-frequency (~2.5 Hz) peak is reduced, that of the one at 5 Hz is unaltered, but the peak at gamma frequency is significantly increased. *C*: autocorrelograms of 1-s sweeps recorded during immobility (*left panel*) and exploration (*right panel*). During immobility, the autocorrelogram is dominated by the low-frequency, breathing-associated rhythmicity (1st peak at 350 ms yielding a frequency of 2.8 Hz). During exploration, there are prominent peaks with ~20 ms separation, indicating a much more pronounced gamma frequency oscillation. The *insets* show the autocorrelograms at an expanded time scale.

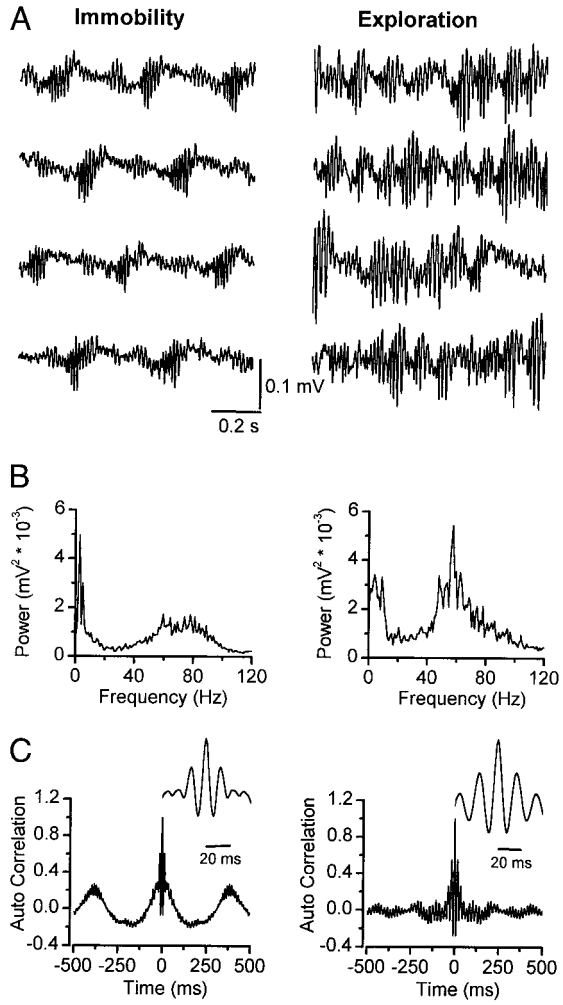

FIG. 5. Increased gamma frequency oscillation in $\beta3-/-$ olfactory bulb. *A*: continuous recordings of electroencephalograms (EEGs) from a $\beta3-/-$ mouse olfactory bulb during immobility (*left panel*) and exploration (*right panel*). During exploration, the EEG is dominated by a high-amplitude, high-frequency rhythm. *B*: the peak at 40–90 Hz is much more pronounced in $\beta3-/-$ mice compared with the controls. There is a decrease in the amplitude of the 3-Hz peak during exploration, without any significant change in the amplitude of the peak at ~5 Hz. In $\beta3-/-$ mice, the gamma frequency peak is also more pronounced during exploration than during immobility. The 2 peaks at ~3 and ~6 Hz are very similar in $\beta3-/-$ mice to those recorded in control animals, but there is a large increase in the power of the gamma frequency band (cf. Fig. 3). *C*: autocorrelograms of 1-s EEGs recorded during immobility (*left panel*) and exploration (*right panel*). Similar to control animals, during immobility the low-frequency activity dominates the autocorrelogram, but the peaks with ~14-ms separation are more pronounced. During exploration, high-amplitude peaks with ~17-ms separation show a very strong gamma frequency activity. The *insets* show the autocorrelograms at an expanded time scale.

3, $P = 0.05$) in $\beta3-/-$ compared with control mice. We also computed autocorrelograms of the EEG and found a very pronounced increase in the peak at 15–25 ms (Figs. 4*C* and 5*C*) consistent with the increased power of gamma frequency band.

In summary, during exploration, the power of both the theta and gamma frequency oscillations increased in the olfactory bulb of $\beta3-/-$ mice. When the animals did not move and did not show any observable sniffing activity, the powers of the theta and gamma frequency oscillations were similar between wild type and $\beta3-/-$ animals. The frequency of the oscillations did not show a prominent alteration in $\beta3-/-$ mice. Taken together, these results show that the almost complete disruption of GABAergic synaptic inhibition of granule cells, and the increased mIPSC amplitude in mitral/tufted cells, results in an enhanced oscillatory power in $\beta3-/-$ olfactory bulb (OB). We next tested the effect of such altered neuronal network oscillations on odor discrimination.

Altered odor discrimination in $\beta3-/-$ mice

A first observation was that the $\beta3-/-$ mice were more active than the $\beta3+/+$ mice, as has been reported elsewhere (Homanics et al. 1997). All animals learned to dig in an odorized dish (geraniol) versus control (mineral oil), which indicates that the $\beta3-/-$ mice can smell.

Odor identification/discrimination was tested with two tasks. The first task was a simple identification of a learned alcohol (hexanol) in a randomly presented series of chemically similar alcohols and a chemically unrelated odorant IAA. The mice were tested two times in the same session on the randomized series of odorants. Time spent digging in a scented dish was used to assess identification and generalization. In the first round of tests, none of the mice showed significant generalization to odorants other than the training odor (Figs. 7, *A* and *B*). In the second round of tests, the $\beta3+/+$ mice generalized to heptanol and dug very little in the other odorants (Fig. 7*C*). The $\beta3-/-$ mice dug significantly only in hexanol, showing no generalization (Fig. 7*D*). Thus with practice, the $\beta3-/-$ mice performed better than the $\beta3+/+$ mice in distinguishing this monomolecular alcohol from closely related alcohols.

The second odor identification test was a more complex mixture identification task. The mice were trained on a mixture of four alcohols and then tested on the original mixture (OM: butanol, pentanol, heptanol, and decanol) and four close mixtures (those consisting of 3 of the original 4 components; M1–M4, see METHODS). They were each tested three times on randomized series of the five mixtures in a single session. In the first round the $\beta3+/+$ mice made no distinction among the odors (Fig. 8*A*), whereas the $\beta3-/-$ mice generalized to those mixtures lacking the long chain components (M3 and M4) and discriminated those mixtures lacking the short chain components (M1 and M2; Fig. 8*B*). In the second round the $\beta3+/+$ mice generalized to one mixture (M4 in Fig. 8*C*), and the $\beta3-/-$ mice generalized across all odor mixtures (Fig. 8*D*). In the third and final round, the $\beta3+/+$ mice correctly distinguished the learned odor from the other mixtures (Fig. 8*E*), and the $\beta3-/-$ mice did as well as the $\beta3+/+$ mice had done on the second round (Fig. 8*F*). While the $\beta3-/-$ mice initially performed better than the $\beta3+/+$ mice on this task, with subsequent exposure to the panel of test odors, they confused the mixtures (*round 2*) and then began to relearn the discrimination (*round 3*). The generalization patterns seen in the mixture identification test suggest that effective concentration may also play a role in performance in both sets of animals. The mixture most readily confused with the training mixture (OM) was that lacking the longest chain, and thus less volatile, alcohol (M4). This alcohol may be less noticed in a mixture of more volatile alcohols and so may participate less in the representation of the OM.

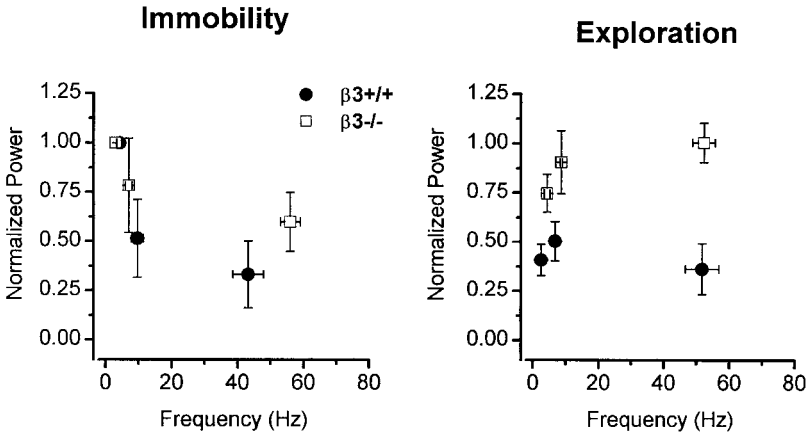

FIG. 6. Comparison of the oscillatory EEG activity in β3+/+ and β3−/− mice. Power spectra were normalized in 4 control (●) and 3 β3−/− (□) mice to the amplitude of the low-frequency peak during immobility. A significant difference ($P < 0.05$, unpaired *t*-test) between control and β3−/− mice was found in the normalized power of both theta and gamma frequency oscillations during exploration. During immobility, there was no significant change in the power or frequency of the oscillations.

DISCUSSION

We have demonstrated a dramatic reduction of synaptic $GABA_A$ receptor–mediated inhibition in GABAergic interneurons (granule cells) of the OB caused by the targeted disruption of the $GABA_A$ receptor β3 subunit gene. Because there was an increase, rather than a decrease, in the mIPSC amplitudes in β3−/− principal cells (mitral and tufted), a cell type–selective abolition of synaptic inhibition was achieved in the olfactory bulb of β3−/− mice. In parallel with these altered patterns of synaptic inhibition, we observed a large increase in the amplitude of olfactory bulb theta and gamma frequency oscillations in vivo during exploration, i.e., while the mice showed intense sniffing activity. In two olfactory discrimination tasks, β3−/− mice showed both an increased ability to discriminate monomolecular alcohols and a decreased ability to discriminate closely related mixtures of alcohols, relative to wild type littermates.

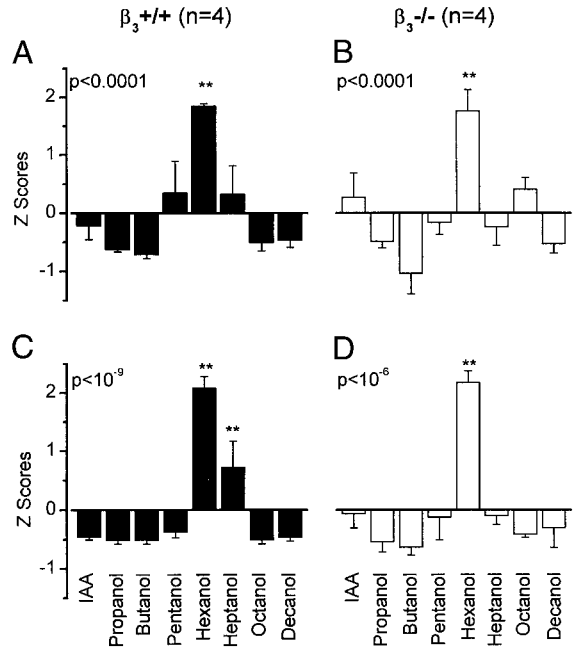

FIG. 7. Alcohol identification task. Results from β3+/+ mice on the *left*, from β3−/− mice on the *right*. The same test was performed twice: *round 1*: *A* and *B*; *round 2*: *C* and *D*. *A* and *B*: β3+/+ and β3−/− mice correctly identify the trained odor, hexanol [significant variation across the set of odors tested with ANOVA; *A*: $F_{(7,24)} = 8.49$, $P < 10^{-4}$; *B*: $F_{(7,24)} = 8.69$, $P < 10^{-4}$]. *C*: β3+/+ mice generalize to heptanol only [$F_{(7,24)} = 26.26$, $P < 10^{-9}$]. *D*: β3−/− mice do not generalize [$F_{(7,24)} = 15.26$, $P < 10^{-6}$]. (** $P <$ 0.01 from a post hoc Newman-Keuls test, indicating the difference between the test odor and all other odors; error bars show standard error of *Z*-scores.) Data are normalized as described in METHODS.

Cell type–selective reduction of synaptic inhibition in the olfactory bulb of β3−/− mice

Examination of the expression of $GABA_A$ receptor subunits in the mammalian brain revealed that most nerve cells express a large variety of subunits (Fritschy and Mohler 1995; Persohn et al. 1992; Wisden et al. 1992), which are co-assembled into several $GABA_A$ receptor subtypes. Even within a single subunit class, most nerve cells express several subunit variants. For example, cortical and hippocampal pyramidal cells, like olfactory bulb mitral cells, express at least three α and three β subunit variants. Thus after genetic deletion of a single subunit, the total elimination of functional $GABA_A$ receptors is not predicted. Less frequently, some neurons express only a single subunit of a given subunit class (Fritschy and Mohler 1995; Persohn et al. 1992; Wisden et al. 1992). For example, granule cells of the olfactory bulb express strongly only the β3 as the β subunit (Nusser et al. 1999b). Because it is impossible to form functional $GABA_A$ receptors without β subunits, we expected to observe a total disappearance of functional $GABA_A$ receptors from granule cells in the β3 subunit's absence. In good agreement with this prediction, we found a dramatic reduction of the muscimol-evoked whole-cell current and the total current mediated by mIPSCs in β3−/− granule cells, without an accompanying decrease of mIPSCs in the principal cells. These results are in excellent agreement with those of a previous study using the β3−/− mice to study the alteration of synaptic inhibition in the thalamus (Huntsman et al. 1999), where neurons of the reticular thalamic nucleus express only β3 as the β subunit, whereas relay neurons in the ventrobasal complex express other β subunits. The amplitude, duration, and frequency of the spontaneous IPSCs were greatly reduced in neurons of the reticular thalamic nucleus of β3−/− mice, but those recorded from the ventrobasal nucleus were unaltered. Our work and that of Huntsman et al. (1999) showed an incomplete loss of functional $GABA_A$ receptors in β3 subunit–expressing cells in β3−/− animals. To test whether a compensatory up-regulation of the β1 or β2 subunits is responsible for the incomplete loss of $GABA_A$ receptors in β3−/− olfactory granule cells, we performed light microscopic immu-

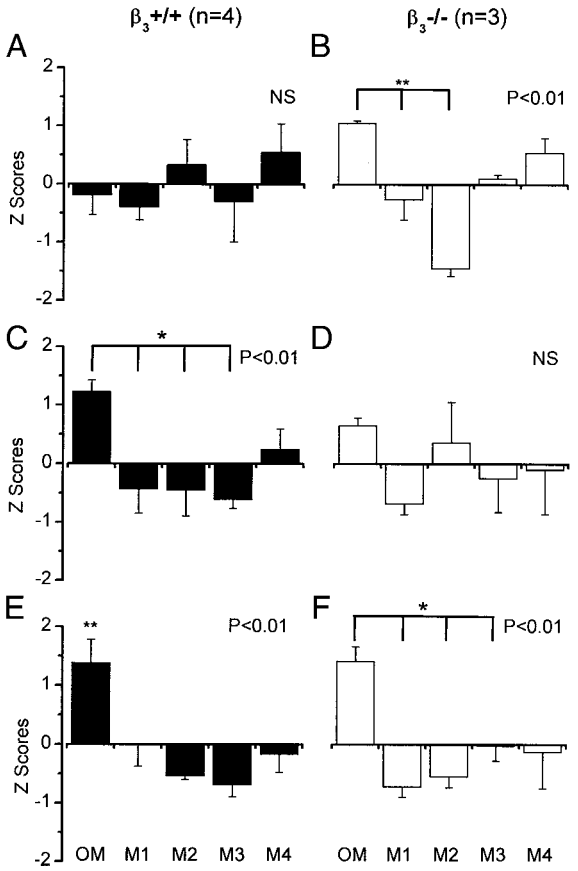

FIG. 8. Alcohol mixture task. Results from the $\beta3+/+$ mice on the *left*, from $\beta3-/-$ mice on the *right*. The test was performed 3 times: *round 1*: *A* and *B; round 2*: *C* and *D; round 3*: *E* and *F*. *A*: $\beta3+/+$ mice generalize across all odor mixtures [$F_{(4,15)} = 0.76$, $P = 0.5680$]. *B*: $\beta3-/-$ mice discriminate the trained mixture (OM) from mixtures M1 and M2 [$F_{(4,10)} = 21.23$, $P < 10^{-4}$; ** post hoc test shows difference between OM and M1 and M2 at $P < 0.01$]. *C*: $\beta3+/+$ mice distinguish between the trained mixture and 3 of the 4 test mixtures [$F_{(4,15)} = 5.12$, $P = 0.0084$; * post hoc difference between OM and M1–M3, $P < 0.05$]. *D*: $\beta3-/-$ mice generalize across all odors [$F_{(4,10)} = 0.94$, $P = 0.4809$]. *E*: $\beta3+/+$ mice correctly identify the learned odor and do not generalize [$F_{(4,15)} = 7.65$, $P = 0.0014$; post hoc pairwise differences, $P < 0.01$]. *F*: $\beta3-/-$ mice identify the learned odor in the same pattern as the $\beta3+/+$ mice did in *round 2* [$F_{(4,10)} = 6.05$, $P = 0.0097$; post hoc differences, $P < 0.05$]. OM, original mixture (butanol, pentanol, heptanol, and decanol); M1, pentanol, heptanol, and decanol; M2, butanol, heptanol, and decanol; M3, butanol, pentanol, and decanol; M4, butanol, pentanol, and heptanol (error bars show SE of the *Z*-scores). Data are normalized as described in METHODS.

nohistochemistry with $\beta1$ and $\beta2$ subunit specific antibodies. Although these antibodies provided strong and specific staining throughout the brain, including the external plexiform layer of the olfactory bulb, no detectable specific immunostaining could be observed in the granule cell layer of $\beta3-/-$ olfactory bulb. Unfortunately, the lack of a protein cannot be concluded from the lack of detectable immunostaining using light microscopic immunohistochemistry. Because we were unable to identify the expression of either the $\beta1$ or $\beta2$ subunits in $\beta3-/-$ granule cells, the reason for the incomplete loss of functional $GABA_A$ receptors remains unknown. It is possible that an as yet unidentified β subunit is expressed in granule cells or that its expression is turned on in $\beta3-/-$ mice. There are two possible explanations of the reduced mIPSC frequency and amplitude in $\beta3-/-$ granule cells. One possibility is that the total number of GABAergic synapses is reduced together with a reduced number of $GABA_A$ receptors in the remaining synapses. This would result in a reduced mIPSC frequency and amplitude and the drastic reduction of the total number of surface $GABA_A$ receptors (as observed with the muscimol experiments). The second possibility is that the total number of synapses is not altered, but the number of $GABA_A$ receptors is drastically reduced in every synapse. In this case the apparent decrease in the frequency would be due to our inability to detect very small synaptic currents, which are mediated by less than four to six receptors. This explanation is also consistent with a large reduction in the total number of surface $GABA_A$ receptors.

Although the $\beta3$ subunit was not present in mitral/tufted cells in $\beta3-/-$ mice, we found an increase rather than a decrease in mIPSC amplitudes recorded from these neurons. Because a compensatory up-regulation of the $\beta1$ or $\beta2$ subunits was not observed by light microscopic immunocytochemistry in $\beta3-/-$ mitral/tufted cells, the reason for this observation is unknown. An increased synaptic concentration of GABA could explain the observed increase in mIPSC amplitudes. Such increased concentration may be achieved by an increase in the GABA content of synaptic vesicles or a change in the geometry of the neuropil surrounding the synapse with altered GABA diffusion/uptake. Furthermore, the conductance of the $GABA_A$ receptors in $\beta3-/-$ mitral cells could also be increased as a consequence of the altered subunit composition. With our experimental approach, we cannot exclude the possibility that the large mIPSCs in $\beta3-/-$ mitral cells are glycinergic synaptic currents. However, this possibility would require that the glycinergic synaptic currents had the same decay kinetics compared with the GABAergic mIPSCs in control (under control conditions, mIPSCs are bicuculline sensitive). Furthermore, as we did not detect a change in the mIPSC frequency, a complex regulation would be required to decrease the GABAergic IPSC frequency in proportion to the appearance of the glycinergic synaptic currents in $\beta3-/-$ mitral cells. Irrespective of the mechanism of the increased mIPSCs in mitral cells, our data show that a *cell type–selective reduction* of synaptic $GABA_A$ receptor–mediated inhibition could be achieved in the $\beta3-/-$ olfactory bulb. However, it is important to point out that in the $\beta3-/-$ mice, we did not find a complete loss of functional $GABA_A$ receptors in granule cells, and we did observe an increase in mIPSC amplitudes in mitral/tufted cells, which could be the consequence of some compensatory mechanisms, as observed in other $GABA_A$ receptor subunit–deleted mice (Brickley et al. 2001; Jones et al. 1997; Nusser et al. 1999a). Future experiments with cell type–specific and inducible knock-out animals will be required to achieve selective elimination of GABAergic inhibition without possible secondary, compensatory effects in the olfactory bulb network.

GABAergic inhibition of granule cells plays a role in oscillatory synchronization in the OB

Oscillatory synchronization in the theta and gamma frequency ranges has been described in several brain regions, including the hippocampus, thalamus, visual cortex, olfactory cortex, and the olfactory bulb. Several studies using experimental and/or modeling approaches pointed to the importance of GABAergic interneurons in the generation of network oscillations (Cobb et al. 1995; Lytton and Sejnowski 1991; Rall

et al. 1966; Singer 1996; Soltesz and Deschenes 1993; Steriade et al. 1993; Traub et al. 1998; von Krosigk et al. 1993; Wang and Buzsaki 1996; Whittington et al. 1995). Models of neocortex, hippocampus, and insect antennal lobe have predicted that synaptically interconnected networks of GABAergic interneurons could generate subthreshold oscillations in principal cells (Bazhenov et al. 2001; Traub et al. 1998; Wang and Buzsaki 1996; Whittington et al. 1995). Some recent studies also pointed to the importance of the electrical coupling between GABAergic local-circuit interneurons in population synchronization (Galarreta and Hestrin 1999; Gibson et al. 1999; Mann-Metzer and Yarom 1999; Tamas et al. 2000). Most olfactory bulb modeling schemes do not include synaptic interactions between GABAergic granule cells (Fukai 1996; Hendin et al. 1997; Li and Hopfield 1989). When these connections are included in OB models, their role in the generation of network oscillations seems to be in disagreement. One model suggests that gamma oscillations arise as a result of negative feedback between excitatory and inhibitory connections and that mutual inhibition serves to desynchronize neurons or decrease the amplitude of oscillations, in agreement with our results (Freeman 1979). Another model suggests that gamma oscillations are produced by mutual inhibition of granule cells (Linster and Gervais 1996). A recent modeling study of oscillatory network activity in the locust antennal lobe, the insect circuit analogous to the vertebrate OB, specifically examined the role of inhibitory connections between inhibitory local neurons (LNs) on circuit dynamics (Bazhenov et al. 2001). In this system, odors evoke distributed activity across PN assemblies whose elements evolve over time in a stimulus-specific manner (Laurent et al. 1996; Wehr and Laurent 1996). An odor is thus normally represented by a temporal succession of transiently synchronized subsets of PNs. Blocking LN-LN inhibitory synapses while sparing LN-PN synapses in the model led to a disappearance of transient synchronization, thus prolonging each PN's participation in the population representation, decreasing the number of desynchronized PNs and increasing the number of participating PNs at each cycle of the oscillatory response (Bazhenov et al. 2001). This observation is consistent with our experimental observation that local field potential gamma-band oscillatory power increased in β3−/− mice. A prediction is therefore that individual mitral cell temporal response patterns should be less precisely defined and more prolonged in β3−/− mutants than in control mice. Independent of the approach and the area studied, most studies seem to agree that $GABA_A$ receptor–mediated chemical synaptic neurotransmission is essential for the generation of fast network oscillations. Furthermore, the essential role of $GABA_A$ receptor–mediated synaptic transmission *between GABAergic interneurons* has been acknowledged, but has not yet been proven experimentally. This is because of the lack of selective deletion/block of $GABA_A$ receptor–mediated transmission between GABAergic interneurons that would spare the excitability/responsiveness of principal cells.

In the olfactory bulb (our study) as well as in the thalamus (Huntsman et al. 1999), the drastically reduced inhibition in GABAergic interneurons resulted in a large increase in the power of network oscillations at the gamma and theta frequency ranges. The observed increase in the frequency and power of the higher frequency theta band, breathing-associated, oscillation in the olfactory bulb may be explained by the increased sniffing rate of the relatively hyperactive β3−/− mice. The mechanisms underlying the increased power of gamma frequency oscillation are unclear, but may include the following: *1*) increased synaptic conductances in mitral/tufted cells; *2*) higher excitability of mitral/tufted cells; *3*) larger numbers of mitral/tufted cells participating in the oscillation; *4*) increased oscillatory coherence between the active principal cells; *5*) altered centrifugal input to the granule cells, resulting in increased synchrony of mitral cells (Gray and Skinner 1988); or *6*) combinations of the above. Future studies on inducible $GABA_A$ receptor knock-out animals with multiunit recordings will be required to elucidate some of the above hypotheses.

An unresolved issue about the circuitry of the mammalian olfactory bulb is the source of GABAergic synapses on granule cells. Previously, we identified two distinct populations of mIPSCs in granule cells and suggested that they may originate from distinct sources (Nusser et al. 1999b). One obvious source is the input from the GABAergic short axon cells present in the granule cell layer (Schneider and Macrides 1978). The second source may be interconnection of granule cells through dendritic synapses. Finally, the basal forebrain (diagonal band nuclei) and, to a lesser extent, the ventral pallidum, anterior amygdala, and the nucleus of the lateral olfactory tract could also provide a GABAergic innervation of the granule cells (Zaborsky et al. 1986). It remains to be determined whether the reduced synaptic inhibition in β3−/− granule cells affects all inputs or just some of them.

Finally, our results showed that with the changes in OB oscillatory synchrony, on behavioral tests the β3−/− mice performed better than their control littermates in identifying a monomolecular alcohol but worse in discriminating–highly overlapping mixtures of alcohols. These differences were dependent on experience with the odors, as in initial tests the β3−/− mice performed the same as the control mice on the single alcohol discrimination test and better than the control mice on the mixture discrimination test. These results indicate that increased network synchrony has a complex effect on odor learning, representation, and discrimination.

It has been shown that oscillating assemblies of projection neurons participate in odor representation and discrimination in the locust antennal lobe (Wehr and Laurent 1996), and it has been suggested that the same may be true of mitral cells in the rabbit olfactory bulb (Kashiwadani et al. 1999). It has also been shown that the coherence of odor-evoked oscillations increases following repeated exposure to odors in locusts (Stopfer and Laurent 1999). If an increase in the number of synchronized mitral cells underlies the increase in gamma power of β3−/− mice, then larger than normal neural cell assemblies (NCAs) may encode a given molecular species in the olfactory bulb mitral cell population, perhaps accompanied by increased separation of the NCAs for chemically related monomolecular odorants. This may be due to an increase in lateral inhibition from granule to mitral cells caused by the decrease in mutual inhibition between granule cells, as suggested by modeling studies (Linster and Gervais 1996; Yokoi et al. 1995) and by the increase in mitral cell mIPSCs that we report here.

An increase in the size or effective power of a NCA could account for both behavioral results reported here. Training on a single monomolecular odorant would in β3−/− mice produce a large NCA representing that odor and could make these

animals specialists for that odor. Experience would then enhance the separation of NCAs more in $\beta3-/-$ than control mice. Training on a mixture of closely related alcohols produces an initial behavioral response that is better for $\beta3-/-$ than control mice, due to the increased size of the NCA. Subsequent experience with the test mixtures produces competing, highly overlapping NCAs, since the test mixtures are very similar in chemical composition and the NCAs representing *monomolecular* odors in $\beta3-/-$ mice are presumed to be larger and more separated than those of control mice. This could explain the decrease in performance of the $\beta3-/-$ mice in the second round of the mixture task. However, the $\beta3-/-$ mice are not so impaired that they cannot eventually learn to discriminate the mixtures, as is indicated by their performance in the third round of tests. It is probable that with further training they could have done as well as their control littermates. It is also possible that prior learning of the monomolecular discrimination task affected subsequent performance in the mixture task differently in the two groups of mice. Because of the small numbers of animals and the difficulty of breeding the $\beta3-/-$ mice, we were unable to test this possibility.

To *prove* the role of network oscillations in odor coding and discrimination, the animals should be first trained in one state (e.g., in control state) and consequently tested in another (e.g., after altered network synchrony). Because we were unable to train and test our "conventional" $\beta3$ subunit–deleted mice in such a way, future experiments with an inducible deletion will be necessary. Such experiments will require precise controls of the effects of the manipulations on the tuning of individual mitral/tufted cells. Such an approach might also allow testing of the lateral inhibition hypothesis for the response tuning of individual mitral/tufted cells (Yokoi et al. 1995).

We thank Dr. Anatol Bragin for help with the in vivo recordings. We are grateful to Dr. Werner Sieghart for providing the $GABA_A$ receptor β subunit-specific antibodies. We also thank C. Ferguson and J. Steinmiller for expert technical assistance with the $\beta3-/-$ animals and Dr. Tamas Freund for comments on the manuscript.

This work was supported by a Wellcome International Travelling Fellowship, a Boehringer Ingelheim Award, and a Hungarian Science Foundation grant to Z. Nusser; a Burroughs-Wellcome fellowship in Computational Molecular Biology to L. M. Kay; National Institutes of Health (NIH) Grants GM-52035 and AA-14022 to G. E. Homanics; and NIH Grants NS-30549 and NS-35985 and the Coelho Endowment to I. Mody.

REFERENCES

ADRIAN ED. Olfactory reactions in the brain of the hedgehog. *J Physiol (Lond)* 100: 459–473, 1942.

ADRIAN ED. The electrical activity of the mammalian olfactory bulb. *Electroencephalogr Clin Neurophysiol* 2: 377–388, 1950.

BAZHENOV M, STOPFER M, RABINOVICH M, HUERTA R, ABARBANEL HDI, SEJNOWSKI TJ, AND LAURENT G. Model of transient oscillatory synchronization in the locust antennal lobe. *Neuron* 30: 553–567, 2001.

BRESSLER SL AND FREEMAN WJ. Frequency analysis of olfactory system EEG in cat, rabbit, and rat. *Electroencephalogr Clin Neurophysiol* 50: 19–24, 1980.

BRICKLEY SG, REVILLA V, CULL-CANDY SG, WISDEN W, AND FARRANT M. Adaptive regulation of neuronal excitability by a voltage-independent potassium conductance. *Nature* 409: 88–92, 2001.

BUZSAKI G AND CHROBAK JJ. Temporal structure in spatially organized neuronal ensembles: a role for interneuronal networks. *Curr Opin Neurobiol* 5: 504–510, 1995.

COBB SR, BUHL EH, HALASY K, PAULSEN O, AND SOMOGYI P. Synchronization of neuronal activity in hippocampus by individual GABAergic interneurons. *Nature* 378: 75–78, 1995.

DELOREY TM, HANDFORTH A, ANAGNOSTARAS SG, HOMANICS GE, MINASSIAN BA, ASATOURIAN A, FANSELOW MS, DELGADO-ESCUETA A, ELLISON GD, AND OLSEN RW. Mice lacking the $\beta3$ subunit of the $GABA_A$ receptor have the epilepsy phenotype and many of the behavioral characteristics of angelman syndrome. *J Neurosci* 18: 8505–8514, 1998.

ENGEL AK, ROELFSEMA PR, FRIES P, BRECHT M, AND SINGER W. Role of the temporal domain for response selection and perceptual binding. *Cereb Cortex* 7: 571–582, 1997.

FREEMAN WJ. *Mass Action in the Nervous System*. New York: Academic, 1975.

FREEMAN WJ. *Quantitative Patterns of Integrated Neural Activity*. Sunderland, MA: Sinauer, 1976.

FREEMAN WJ. Nonlinear dynamics of paleocortex manifested in the olfactory EEG. *Biol Cybern* 35: 21–37, 1979.

FRITSCHY J-M AND MOHLER H. $GABA_A$-receptor heterogeneity in the adult rat brain: differential regional and cellular distribution of seven major subunits. *J Comp Neurol* 359: 154–194, 1995.

FUKAI T. Bulbocortical interplay in olfactory information processing via synchronous oscillations. *Biol Cybern* 74: 309–317, 1996.

GALARRETA M AND HESTRIN S. A network of fast-spiking cells in the neocortex connected by electrical synapses. *Nature* 402: 72–75, 1999.

GELPERIN A AND TANK DW. Odour-modulated collective network oscillations of olfactory interneurons in a terrestrial mollusc. *Nature* 345: 437–440, 1990.

GIBSON JR, BEIERLEIN M, AND CONNORS BW. Two networks of electrically coupled inhibitory neurons in neocortex. *Nature* 402: 75–79, 1999.

GRAY CM AND SINGER W. Stimulus specific neuronal oscillations in orientation columns of cat visual cortex. *Proc Natl Acad Sci USA* 86: 1698–1702, 1989.

GRAY CM AND SKINNER JE. Centrifugal regulation of neuronal activity in the olfactory bulb of the walking rabbit as revealed by reversible cryogenic blockade. *Exp Brain Res* 69: 378–386, 1988.

HAJOS N, NUSSER Z, RANCZ EA, FREUND TF, AND MODY I. Cell type- and synapse-specific variability in synaptic $GABA_A$ receptor occupancy. *Eur J Neurosci* 12: 810–818, 2000.

HENDIN O, HORN D, AND TSODYKS MV. The role of inhibition in an associative memory model of the olfactory bulb. *J Comput Neurosci* 4: 173–182, 1997.

HOMANICS GE, DELOREY TM, FIRESTONE LL, QUINLAN JJ, HANDFORTH A, HARRISON NL, KRASOWSKI MD, RICK CE, KORPI ER, MAKELA R, BRILLIANT MH, HAGIWARA N, FERGUSON C, SNYDER K, AND OLSEN RW. Mice devoid of γ-aminobutyrate type A receptor $\beta3$ subunit have epilepsy, cleft palate, and hypersensitive behavior. *Proc Natl Acad Sci USA* 94: 4143–4148, 1997.

HUNTSMAN MM, PORCELLO DM, HOMANICS GE, DELOREY TM, AND HUGUENARD JR. Reciprocal inhibitory connections and network synchrony in the mammalian thalamus. *Science* 283: 541–543, 1999.

JECHLINGER M, PELZ R, TRETTER V, KLAUSBERGER T, AND SIEGHART W. Subunit composition and quantitative importance of hetero-oligomeric receptors: $GABA_A$ receptors containing $\alpha6$ subunits. *J Neurosci* 18: 2449–2457, 1998.

JONES A, KORPI ER, MCKERNAN RM, PELZ R, NUSSER Z, MAKELA R, MELLOR JR, POLLARD S, BAHN S, STEPHENSON FA, RANDALL AD, SIEGHART W, SOMOGYI P, SMITH AJ, AND WISDEN W. Ligand-gated ion channel subunit partnerships: $GABA_A$ receptor $\alpha6$ subunit gene inactivation inhibits d subunit expression. *J Neurosci* 17: 1350–1362, 1997.

KASHIWADANI H, SASAKI YF, UCHIDA N, AND MORI K. Synchronized oscillatory discharges of mitral/tufted cells with different molecular receptive ranges in the rabbit olfactory bulb. *J Neurophysiol* 82: 1786–1792, 1999.

KAY LM, CHIANG E, LY K, LAURENT G, AND SMITH BH. Evaluation of olfactory learning and generalization in C57BL6 mice. *Soc Neurosci Abstr* 26: 2245, 2000.

KAY LM AND FREEMAN WJ. Bidirectional processing in the olfactory-limbic axis during olfactory behavior. *Behav Neurosci* 112: 541–553, 1998.

LAURENT G AND DAVIDOWITZ H. Encoding of olfactory information with oscillating neural assemblies. *Science* 265: 1872–1875, 1994.

LAURENT G, WEHR M, AND DAVIDOWITZ H. Temporal representations of odors in an olfactory network. *J Neurosci* 16: 3837–3847, 1996.

LAURIE DJ, SEEBURG PH, AND WISDEN W. The distribution of 13 $GABA_A$ receptor subunit mRNAs in the rat brain. II. Olfactory bulb and cerebellum. *J Neurosci* 12: 1063–1076, 1992.

LI Z AND HOPFIELD JJ. Modeling the olfactory bulb and its neural oscillatory processings. *Biol Cybern* 61: 379–392, 1989.

LINSTER C AND GERVAIS R. Investigation of the role of interneurons and their modulation by centrifugal fibers in a neural model of the olfactory bulb. *J Comput Neurosci* 3: 225–246, 1996.

LINSTER C AND HASSELMO ME. Behavioral responses to aliphatic aldehydes can be predicted from known electrophysiological responses of mitral cells in the olfactory bulb. *Physiol Behav* 66: 497–502, 1999.

LYTTON WW AND SEJNOWSKI TJ. Simulations of cortical pyramidal neurons synchronized by inhibitory interneurons. *J Neurophysiol* 66: 1059–1079, 1991.

MACLEOD K, BACKER A, AND LAURENT G. Who reads temporal information contained across synchronized and oscillatory spike trains? *Nature* 395: 693–698, 1998.

MACLEOD K AND LAURENT G. Distinct mechanisms for synchronization and temporal patterning of odor-encoding neural assemblies. *Science* 274: 976–979, 1996.

MANN-METZER P AND YAROM Y. Electrotonic coupling interacts with intrinsic properties to generate synchronized activity in cerebellar networks of inhibitory interneurons. *J Neurosci* 19: 3298–3306, 1999.

NUSSER Z, AHMAD Z, TRETTER V, FUCHS K, WISDEN W, SIEGHART W, AND SOMOGYI P. Alterations in the expression of $GABA_A$ receptor subunits in cerebellar granule cells after the disruption of the $\alpha 6$ subunit gene. *Eur J Neurosci* 11: 1685–1697, 1999a.

NUSSER Z, ROBERTS JDB, BAUDE A, RICHARDS JG, SIEGHART W, AND SOMOGYI P. Immunocytochemical localization of the $\alpha 1$ and $\beta 2/3$ subunits of the $GABA_A$ receptor in relation to specific GABAergic synapses in the dentate gyrus. *Eur J Neurosci* 7: 630–646, 1995.

NUSSER Z, SIEGHART W, AND MODY I. Differential regulation of synaptic $GABA_A$ receptors by cAMP-dependent protein kinase in mouse cerebellar and olfactory bulb neurones. *J Physiol (Lond)* 521: 421–435, 1999b.

PERSOHN E, MALHERBE P, AND RICHARDS JG. Comparative molecular neuroanatomy of cloned $GABA_A$ receptor subunits in the rat CNS. *J Comp Neurol* 326: 193–216, 1992.

RALL W, SHEPHERD GM, REESE TS, AND BRIGHTMAN MW. Dendrodendritic synaptic pathway for inhibition in the olfactory bulb. *Exp Neurol* 14: 44–56, 1966.

SCHNEIDER SP AND MACRIDES F. Laminar distributions of interneurons in the main olfactory bulb of the adult hamster. *Brain Res Bull* 3: 73–82, 1978.

SINGER W. The changing face of inhibition. *Curr Biol* 6: 395–397, 1996.

SLANY A, ZEZULA J, TRETTER V, AND SIEGHART W. Rat $\beta 3$ subunits expressed in human embryonic kidney 293 cells form high affinity [^{35}S]t-butylbicyclophosphorothionate binding sites modulated by several allosteric ligands of γ-aminobutyric acid type A receptors. *Mol Pharmacol* 48: 385–391, 1995.

SOLTESZ I AND DESCHENES M. Low-frequency and high-frequency membrane potential oscillations during theta activity in CA1 and CA3 pyramidal neurons of the rat hippocampus under ketamine-xylazine anesthesia. *J Neurophysiol* 70: 97–116, 1993.

SOMOGYI P, TAKAGI H, RICHARDS JG, AND MOHLER H. Subcellular localization of benzodiazepine/$GABA_A$ receptors in the cerebellum of rat, cat, and monkey using monoclonal antibodies. *J Neurosci* 9: 2197–2209, 1989.

STERIADE M, MCCORMICK DA, AND SEJNOWSKI TJ. Thalamocortical oscillations in the sleeping and aroused brain. *Science* 262: 679–685, 1993.

STOPFER M, BHAGAVAN S, SMITH BH, AND LAURENT G. Impaired odour discrimination on desynchronization of odour-encoding neural assemblies. *Nature* 390: 70–74, 1997.

STOPFER M AND LAURENT G. Short-term memory in olfactory network dynamics. *Nature* 402: 664–668, 1999.

TAMAS G, BUHL EH, LORINCZ A, AND SOMOGYI P. Proximally targeted GABAergic synapses and gap junctions synchronize cortical interneurons. *Nature Neurosci* 3: 366–371, 2000.

TRAUB RD, SPRUSTON N, SOLTESZ I, KONNERTH A, WHITTINGTON MA, AND JEFFERYS GR. Gamma-frequency oscillations: a neuronal population phenomenon, regulated by synaptic and intrinsic cellular processes, and inducing synaptic plasticity. *Prog Neurobiol* 55: 563–575, 1998.

TRAUB RD, WHITTINGTON MA, STANFORD IM, AND JEFFERYS JGR. A mechanism for generation of long-range synchronous fast oscillations in the cortex. *Nature* 383: 621–624, 1996.

VON KROSIGK M, BAL T, AND MCCORMICK DA. Cellular mechanisms of a synchronized oscillation in the thalamus. *Science* 261: 361–364, 1993.

WANG X-J AND BUZSAKI G. Gamma oscillation by synaptic inhibition in a hippocampal interneuronal network model. *J Neurosci* 16: 6402–6413, 1996.

WEHR M AND LAURENT G. Odour encoding by temporal sequences of firing in oscillating neural assemblies. *Nature* 384: 162–166, 1996.

WHITTINGTON MA, TRAUB RD, AND JEFFERYS JGR. Synchronised oscillations in interneuron networks driven by metabotropic glutamate receptor activation. *Nature* 373: 612–615, 1995.

WISDEN W, LAURIE DJ, MONYER H, AND SEEBURG PH. The distribution of 13 $GABA_A$ receptor subunit mRNAs in the rat brain. I. Telencephalon, diencephalon, mesencephalon. *J Neurosci* 12: 1040–1062, 1992.

YOKOI M, MORI K, AND NAKANISHI S. Refinement of odor molecule tuning by dendrodendritic synaptic inhibition in the olfactory bulb. *Proc Natl Acad Sci USA* 92: 3371–3375, 1995.

ZABORSZKY L, CARLSEN J, BRASHEAR HR, AND HEIMER L. Cholinergic and GABAergic afferents to the olfactory bulb in the rat with special emphasis on the projection neurons in the nucleus of the horizontal limb of the diagonal band. *J Comp Neurol* 243: 488–509, 1986.